

Medical Physics Contribution:

Commissioning of small field size radiosurgery cones in a 6-MV flattening filter-free beam



Juan Diego Azcona, Ph.D.,^{*†} Benigno Barbés, Ph.D.,^{*†} Verónica Morán, M.S.,^{*} and Javier Burguete, Ph.D.^{†‡}

^{*}Clínica Universidad de Navarra, Department of Radiation Physics, Avenida Pío XII, 31080, Pamplona, Navarra, Spain; [†]IdiSNA, Instituto de Investigación Sanitaria de Navarra, Pamplona, Navarra, Spain; and [‡]Universidad de Navarra, School of Sciences, Department of Physics and Applied Mathematics, Calle Iruñlarrea, 31080, Pamplona, Navarra, Spain

ARTICLE INFO

Article history:

Received 26 October 2016

Received in revised form 25 May 2017

Accepted 16 June 2017

Keywords:

Radiosurgery

Small fields

Flattening filter free

Transmission chamber

ABSTRACT

This study aimed to describe the commissioning of small field size radiosurgery cones in a 6-MV flattening filter free (FFF) beam and report our measured values. Four radiosurgery cones of diameters 5, 10, 12.5, and 15 mm supplied by Elekta Medical were commissioned in a 6-MV FFF beam from an Elekta Versa linear accelerator. The extraction of a reference signal for measuring small fields in scanning mode is challenging. A transmission chamber was attached to the lower part of the collimators and used for percentage depth dose (PDD) and profile measurements in scanning mode with a stereotactic diode. Tissue-maximum ratios (TMR) and output factors (OF) for all collimators were measured with a stereotactic diode (IBA). TMR and the OF for the largest collimator were also acquired on a polystyrene phantom with a microionization chamber of 0.016 cm³ volume (PTW Freiburg PinPoint 3D). Measured TMR with diode and PinPoint microionization chamber agreed very well with differences smaller than 1% for depths below 20 cm, except for the smaller collimator, for which differences were always smaller than 2%. Calculated TMR were significantly different (up to 7%) from measured TMR. OF measured with diode and chamber showed a difference of 3.5%. The use of a transmission chamber allowed the measurement of the small-field dosimetric properties with a simple setup. The commissioning of radiosurgery cones in FFF beams has been performed with essentially the same procedures and recommended detectors used with flattened beams. Good agreement was found between TMR measurements acquired with the IBA stereotactic diode and the PinPoint 3D microionization chamber. The transmission chamber overcomes the problem of extracting a reference signal and is of great help for small-field commissioning.

© 2017 American Association of Medical Dosimetrists.

Reprint requests to Juan Diego Azcona, Ph.D., Clínica Universidad de Navarra, Department of Radiation Physics, Avda. Pío XII, 36, 31080 Pamplona, Navarra, Spain.

E-mail: jazcona@unav.es

<https://doi.org/10.1016/j.meddos.2017.06.003>

0958-3947/Copyright © 2017 American Association of Medical Dosimetrists

Introduction

Small-field measurements and their characterization in treatment planning systems (TPS) are challenging dosimetry tasks. Small fields exhibit singular properties such as the lack of electronic equilibrium and the partial occlusion

of the beam primary source.^{1,2} In addition to this, the measurement of small field size percentage depth-dose (*PDD*) curves, tissue-phantom ratios (*TPR*), profiles, and output factors (*OF*) for dose calculations in TPS is complicated owing to the finite volume of the detector, whose size is comparable (*i.e.*, non-negligible) with the size of the beam, and also because of the density of the detector volume, which may be very different from the medium in which the measurements are taken, usually water.^{1,2} These 2 effects result in a perturbation of the beam characteristics to be measured. The differences in density affect the level of charged-particle equilibrium, and the finite volume leads to an averaging of the signal. This is the case for 2 commonly used small-field detectors: air-filled microionization chambers and silicon diodes.

The influence of these 2 effects on the response of a detector depends on the field size.^{3,4} Currently, there is ongoing research in the scientific community to determine Monte Carlo-based correction factors for specific detectors to remove the combined finite size and material effect of the detector on the measurements.^{4–6} However, there are not any published recommendations yet on how to carry out these corrections. Several documents providing recommendations of good practice^{2,7,8} have different recommendations on the use of the diode, ionization chamber, and radiochromic film for relative measurements in small fields. American Association of Physicists in Medicine TG-106⁷ gives a general statement for the use of microionization chambers in these measurements, whereas European Society for Radiotherapy and Oncology Booklet n. 9⁸ advises the use of diodes and diamonds. It is worth noting that both recommendations are based on the small volume of these detectors. Institute of Physics and Engineering in Medicine (IPEM) Report 103² recommends the use of diodes because of their smaller volume for profile and *OF* measurements. For depth dose and tissue-maximum ratio (*TMR*) measurements, IPEM Report 103² accepts the use of both microionization chambers and diodes, as well as radiochromic film, the latter in spite of the complexity of its handling.

Practical issues often hinder the data acquisition. Quite often a scanning device (*i.e.*, a water tank) is used for performing these measurements. Careful alignment with the beam is crucial to ensure that the detector is located in the center of the beam (crossline variations would lead to a significant decrease in signal that may affect *OF* and profile measurements) as well as with the radiation beam axis (a misalignment would also affect the *PDD* measurements). Furthermore, a reference signal is needed to remove the pulsed beam fluctuations. An important problem that arises when scanning small fields is the extraction of a reference signal to remove the noise in the measurement. The presence of an additional detector to get a reference signal perturbs the beam incident to the field detector in such small-size cones. Moreover, in our configuration, the collimators are directly attached to the head assembly, leaving no space to introduce a detec-

tor probe to extract a reference signal directly from the linear accelerator (linac) that could be interpreted by the scanning system electrometer. To overcome this problem, a novel transmission chamber has been recently developed that can be set at the collimator exit without altering the relative energy fluence exiting the linac's head and collimator assembly.

The purpose of this work is to describe the commissioning of small field size radiosurgery cones in flattening filter-free (FFF) beams and report our measured values. Measurements of beam *OF*, profiles, and *TMR* obtained with microionization chamber and diode, as well as calculated from measured *PDD* obtained with diode, are reported. The measurement of these quantities needs to be carried out with great care, so we will discuss advantages and drawbacks of different approaches, comparing their respective results.

Methods

A set of 4 circular collimators with diameters of 5, 10, 12.5, and 15 mm was commissioned on an Elekta Versa linac (Elekta Medical, Crawley, UK). The collimators were also manufactured and supplied by Elekta Medical. An FFF beam with a 6-MV nominal energy ($TPR_{20,10} = 0.673$) was used because of its high dose rate (1200 monitor units per minute). The jaws positioning was set to 2×2 cm² for the 4 collimators.

Our purpose was to obtain the set of measurements required by the BrainLab iPlan software for treatment planning on patient radiological images, which consist on a series of *TMR*, *OF*, and profiles. Additionally, *PDD* curves were measured. To achieve this aim, we used a Scanditronix RFA300 water tank (IBA Dosimetry, Schwarzenbruck, Germany) with a Scanditronix stereotactic diode to get *OF*, *PDD* curves, profiles, and *TMR*. Lechner *et al.*⁶ investigated the use of several small-size detectors for the dosimetry of FFF beams. They did not resolve any significant difference in the performance of the 2 detectors used in this study when applied to FFF beams instead of flattened beams. They found the lower correction factors for unshielded diodes (as is the case of the stereotactic diode used in this study) and diamond detectors so they recommend its use for small-field dosimetry based on an expected lower uncertainty.

A novel transmission chamber developed by IBA (Stealth Chamber, IBA Dosimetry) was used to get a reference signal, when using the water tank in scanning mode. The use of the chamber avoids perturbing significantly the energy fluence in a small field by using a reference detector such as ionization chamber or diode that is located in the radiation field. The chamber is filled with air between 2 plastic plates. It is located at the exit of the small-field beam (Fig. 1). The characteristics of the Stealth Chamber and its application as a reference detector for dosimetry have been studied by Gersh.⁹ For the sake of its effect on the beam output, its attenuation on the intensity is very small, (the transmission for a

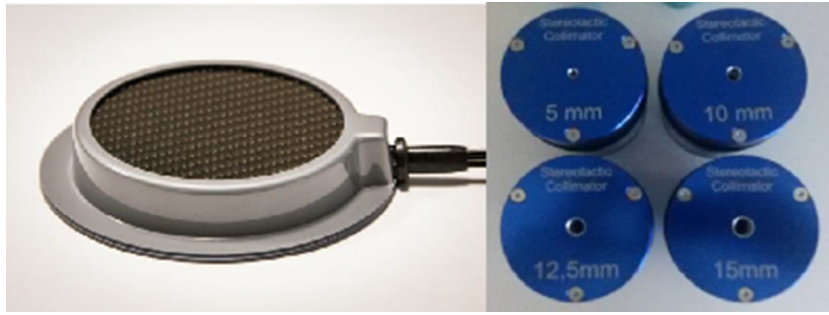


Fig. 1. Stealth ionization chamber and set of cones. When taking measurements, the chamber is attached and fixed to the lower edge of the cones.

0.5 × 0.5 cm² field size is 98%), and does not affect the energy fluence distribution.⁹

PDD curves and profiles were obtained in scanning mode, so the stereotactic diode was used in combination with the Stealth transmission chamber to obtain a reliable reference signal to remove noise in the linac's pulsed beam signal (Fig. 1). *OF* and *TMR* curves were obtained by integrating the measured signal. In all setups, the Stealth Chamber was used in combination with the stereotactic diode to acquire 2 orthogonal profiles in scanning mode and correct the positioning offset from the center of the radiation field, to properly align the stereotactic diode with the beam axis. The stereotactic diode detector was always positioned to ensure that the nominal depth corresponded to the effective diode's point of measurement (0.6 mm downward from its top).

Percentage depth-dose curves

PDD curves were measured at source-to-surface distance (*SSD*) of 98.5 cm and normalized to 100% at 1.5-cm depth. These measurements required a detector centering. This was done at 2 different depths, one at the depth of the maximum and the other at a depth of 25 cm. Ensuring good centering at these 2 depths allows one to quantify the deviation of the detector from the beam axis throughout the range of measurements. This procedure is recommended by IPEM Report 103.² Data were obtained at depths between 0 and 30 cm, every millimeter between 0- and 5-cm depth, and every 5 mm between 5- and 30-mm depth. We used the stereotactic diode because of its smaller volume than the PinPoint microionization chamber. Furthermore, the diode can be easily centered with 2 orthogonal profiles because of its circular symmetry. According to IPEM Report 103,² stereotactic diodes are appropriate detectors for *PDD* measurements.

Tissue-maximum ratios

An accurate centering of the detector is crucial to measure the signal; small deviations from the field center can result in a significant loss of charge that would affect the *TMR* ratios. Because in this quantity the detector lied on a fixed posi-

tion, its centering was defined according to the radiation field, by correcting the offsets determined by 2 orthogonal cross profiles in the plane where the detector was positioned. *TMR* were measured at depths of 0, 5, 8, 12, 14, 15, 16, 18, 20, 25, 30, 40, 50, 60, 75, 100, 125, 150, 175, 200, 225, and 250 mm. Similar to the *PDD* measurements, we used the diode because of its small volume as well as for its ability to be easily centered with the radiation field.

TMR were also measured using a PinPoint 3D microionization chamber, with a 0.016 cm³ volume (PTW Freiburg, Germany). In this case, the measuring medium was a "solid water" polystyrene phantom (PTW Freiburg model 29672, made of slabs of 30 × 30 cm² with different thicknesses ranging from 0.1 to 1 cm). The centering was done according to the cross lines marked in the slab with the chamber holder. *TMR* were measured at the same depths as the stereotactic diode, except 0 mm. The detector was positioned to ensure that the nominal depth corresponded to the effective chamber's point of measurement (1 mm upward from its geometrical center). Although stereotactic diodes are also recommended by IPEM Report 103,² this document's first choice of detectors for *TMR* measurements are microionization chambers. This is justified because, in spite of its larger volume, the detector is always seeing the same jaw opening, so there is no change in the detector response with respect to the field size.

TMR measured with stereotactic diode and PinPoint microionization chamber were compared. Furthermore, *TMR* measured with diode were compared with those calculated from the *PDD* curves measured with diode. *PDD* can be converted to *TMR* according to the classical formula derived by Khan *et al.*^{10,11}:

$$TMR(d, A_d) = \frac{PDD\left(d, A_d \times \frac{SAD}{SSD + d}, SSD\right)}{100} \times \left(\frac{SSD + d}{SAD}\right)^2 \times \frac{S_p(A_{d_{max}})}{S_p(A_d)} \quad (1)$$

where d was the calculation depth at isocenter, A_d was the field size at isocenter, SAD was the source-to-axis (isocenter) distance (100 cm), d_{max} was the depth of the maximum

absorbed dose (1.5 cm), S_p was the phantom-scatter factor, and $A_{d_{max}}$ was the field size at the depth of the maximum. In the *PDD* notation in Eq. (1), we assumed that the field size was specified not at the surface of the phantom but at *SAD*, so it was the nominal cone field size. $A_{d_{max}}$ was related to the nominal field size at isocenter through $A_{d_{max}} = A_d \times \frac{SSD}{SSD + d}$.

It can be seen in Eq. (1) that interpolation of *PDD* among field sizes was needed. In particular, this conversion formula required measured *PDD* and S_p data for the calculation of the *TMR* for the smallest and the largest cones that were not available. Because of this drawback, BrainLab suggested using an approximation to Eq. (1):

$$TMR(d, A_d) = \frac{PDD(d, A_d, SSD)}{100} \times \left(\frac{SSD + d}{SAD} \right)^2 \quad (2)$$

where A_d was the cone field size specified at isocenter. This equation was used in our calculations, and its accuracy for small-field calculations was examined.

Profiles and output factors

Stereotactic diodes are the detector of choice for measuring profiles because of their lower volume that results in a better characterization of the beam penumbra.^{2,8} Profiles were scanned at crossplane and inplane directions with the aid of the Stealth Chamber at a depth of 7.5 cm, once the detector was properly centered with the radiation beam to have a zero offset in both directions. The scanning spatial resolution was 0.5 mm. The radial profile resulting from averaging the 2 sides of each profile and the 2 profiles was used for beam characterization in the BrainLab iPlan TPS.

OF were measured with the stereotactic diode because of its less volume effect that results in a lower variation of the detector response with the radiation field size, for small fields.^{2,8} This is also the advice of Francescon *et al.*⁴ and Lechner *et al.*,⁶ although they recommend using a Monte Carlo-derived correction factor. The measurements were acquired by integrating the electrical charge generated by the radiation beam in the diodes. The Stealth Chamber was used to help with the detector positioning in the center of the radiation field. The center was determined by scanning 2 orthogonal profiles. *OF* were measured at an *SSD* of 98.5 cm and a depth of 1.5 cm in water, and normalized to a 5×5 cm² field. The *OF* of a 5×5 cm² field with respect to a 10×10 cm² field was measured with a Semiflex ionization chamber (0.125 cm³ of volume). The product of both quantities was the final *OF* required by the TPS. This approach is also recommended in Ref. 2. We did not use a Monte Carlo correction factor because of its unavailability in published recommendations from scientific associations on small-field dosimetry. To compare with, we also measured the *OF* of the largest collimator (15 mm diameter) with the PinPoint 3D microionization chamber.

Results

Percentage depth-dose curves and tissue-maximum ratios

Fig. 2 shows the calculated *TMR* based on these *PDD*, as well as the *TMR* measured with the stereotactic diode in water and with the PinPoint microionization chamber in polystyrene for each of the 4 cones. *TMR* values measured with stereotactic diode and PinPoint microionization chamber are provided in Tables 1 and 2, respectively. Comparisons between the 2 sets of measured *TMR* are provided in Table 3. Both sets of measured *TMR* agree quite well. Except in the buildup area, differences for these sets of measurements are slightly above 1% only for large depths (20 cm or more), for all cones but the smallest one. In this cone, differences are below 1% for depths under 10 cm and below 2% for depths up to 25 cm. Differences in the buildup area are attributed to limitations in the detectors used. The volume effect of the ionization chambers affects the measured signal in the buildup region, where there is lack of electronic equilibrium.

Differences between calculated and measured *TMR* are quite large, as can also be seen in Table 4. Except in the buildup area, the differences when using the formula are above 2% for depths of 10 cm and larger, reaching differences larger than 5% for depths around 20 cm and more. This is attributed to 3 reasons. First, as the *PDD* are measured with a depth scanning system, the jaw opening seen by the detector changes, and so it changes its response to the incident beam³ mainly owing to volume averaging but potentially also owing to other perturbation factors. This change of response is particularly accentuated for very small-size fields, and is more pronounced as the nominal field is smaller, as can be seen in the presented data. Second, neglecting the ratio of phantom-scatter factors also has an impact on the outcome of applying the formula, because its variation is also more pronounced for small fields and so its ratio cannot be neglected without leading to a significant error. This approximation leads to an error that increases with depth (strictly speaking, with distance *SSD* + *d* departing *SAD*), according to the ratio of phantom-scatter factors in Eq. (1). This ratio increases with depth as the field size $A_{d_{max}}$ changes with respect to the field size at the isocenter A_d . Third, the use of a single *PDD* curve to calculate a *TMR* curve instead of interpolating the *PDD* required values for each depth for calculation (approximation for the *PDD* values in Eq. 2) also has an impact on the calculations. This approximation also leads to an error that increases at smaller field sizes and larger depths.

Profiles and output factors

Profiles and *OF* were acquired with the stereotactic diode. Table 5 shows the *OF* values. The 15-mm collimator field *OF*

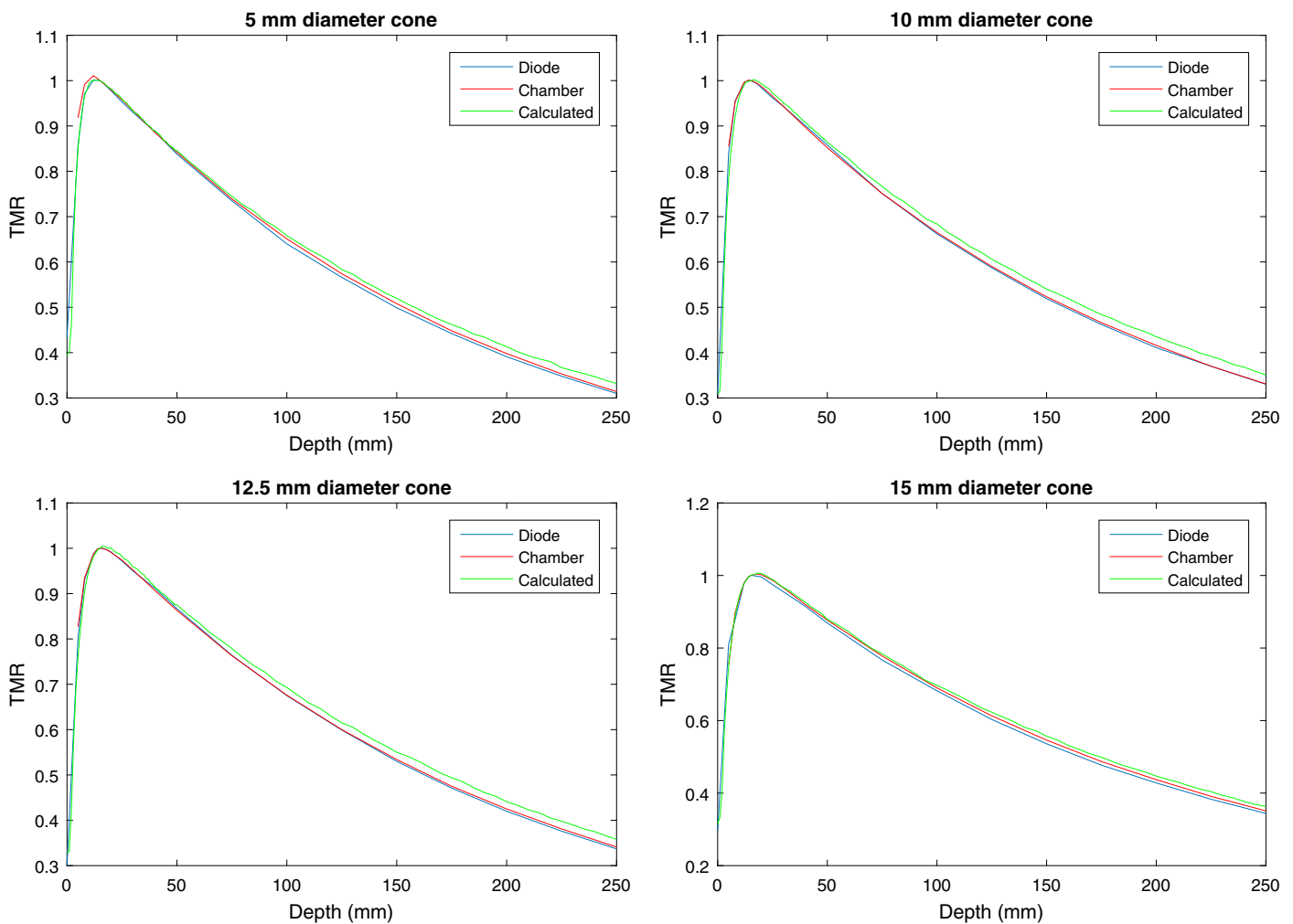


Fig. 2. TMR measured with stereotactic diode and PinPoint microionization chamber and calculated from PDD measurements for each one of the cones.

measured with the PinPoint microionization chamber resulted in a 3.5% lower value with respect to the stereotactic diode measurement, which we attributed to the higher volume effect that results in a change of response with the field size.

Discussion

Small-field measurements are cumbersome, and there are several issues that result in that there is no perfect detector to measure them. There are several recommendations by different organizations.^{2,7,8} Among these, it is always good practice to measure the dosimetric properties with different detectors and to compare them.

An associated problem is the difficulty to extract a good reference signal to remove noise in the signal when measuring in scanning mode, because the reference detector perturbs the small beam incident on the field measuring detector. The scanning mode is appropriate both for centering and for aligning properly the detector with the field axis, as well as for taking PDD and profiles faster in comparison with

acquiring point-by-point measurements and integrating the signal. We have used a Stealth transmission chamber that overcomes this problem. The chamber reads the ionization in a large volume of air filled between 2 thin plastic plates. It is located at the exit of the cone. The transmission of the whole system is very high so it does not perturb significantly the energy fluence exiting the cone.

Our commissioning data correspond to an FFF beam. Same procedures and measuring recommendations as those applied for small fields in flattened beams were followed. The work of Lechner *et al.*⁶ investigated the use of several detectors employed for small-field dosimetry in the context of FFF beams. For the 2 detectors employed in our commissioning, the stereotactic diode and the PinPoint 3D microionization chamber, they found that any different response in FFF beams with respect to flattened beams was within the measurement uncertainty.

Both microionization chambers and stereotactic diodes are recommended detectors for acquiring TMR and PDD. Although measuring PDD is faster than measuring TMR,

Table 1

Tissue-maximum ratios measured with stereotactic diode for each 1 of the 4 cones.

| Depth (mm) | Tissue-maximum ratios measured with diode | | | |
|------------|---|-------|---------|-------|
| | 5 mm | 10 mm | 12.5 mm | 15 mm |
| 0 | 0.434 | 0.308 | 0.300 | 0.296 |
| 5 | 0.858 | 0.840 | 0.802 | 0.811 |
| 8 | 0.971 | 0.956 | 0.930 | 0.879 |
| 12 | 1.001 | 0.995 | 0.988 | 0.979 |
| 14 | 1.001 | 1.000 | 0.999 | 0.996 |
| 15 | 1.000 | 1.000 | 1.000 | 1.000 |
| 16 | 0.997 | 0.998 | 1.000 | 1.000 |
| 18 | 0.987 | 0.993 | 0.997 | 0.998 |
| 20 | 0.978 | 0.984 | 0.992 | 0.996 |
| 25 | 0.953 | 0.962 | 0.972 | 0.975 |
| 30 | 0.930 | 0.943 | 0.950 | 0.955 |
| 40 | 0.887 | 0.901 | 0.912 | 0.915 |
| 50 | 0.838 | 0.858 | 0.867 | 0.869 |
| 75 | 0.735 | 0.751 | 0.764 | 0.767 |
| 100 | 0.640 | 0.662 | 0.675 | 0.682 |
| 125 | 0.566 | 0.587 | 0.599 | 0.603 |
| 150 | 0.499 | 0.519 | 0.530 | 0.536 |
| 175 | 0.442 | 0.462 | 0.471 | 0.477 |
| 200 | 0.391 | 0.411 | 0.420 | 0.428 |
| 225 | 0.348 | 0.370 | 0.376 | 0.383 |
| 250 | 0.310 | 0.330 | 0.337 | 0.344 |

calculated *TMR* tables from measured *PDD* curves are less reliable because of the reasons examined in the Results section. Therefore, calculating *TMR* from measured *PDD* in small-size cones is strongly discouraged.²

Table 2

Tissue-maximum ratios measured with microionization chamber for each 1 of the 4 cones.

| Depth (mm) | Tissue-maximum ratios measured with chamber | | | |
|------------|---|-------|---------|-------|
| | 5 mm | 10 mm | 12.5 mm | 15 mm |
| 5 | 0.918 | 0.855 | 0.827 | 0.817 |
| 8 | 0.992 | 0.954 | 0.935 | 0.928 |
| 12 | 1.011 | 0.996 | 0.987 | 0.986 |
| 14 | 1.004 | 1.001 | 0.999 | 0.998 |
| 15 | 1.000 | 1.000 | 1.000 | 1.000 |
| 16 | 0.996 | 0.999 | 1.000 | 1.001 |
| 18 | 0.989 | 0.994 | 0.997 | 1.000 |
| 20 | 0.980 | 0.987 | 0.991 | 0.995 |
| 25 | 0.958 | 0.966 | 0.974 | 0.978 |
| 30 | 0.934 | 0.943 | 0.952 | 0.957 |
| 40 | 0.886 | 0.897 | 0.907 | 0.912 |
| 50 | 0.842 | 0.852 | 0.863 | 0.868 |
| 75 | 0.739 | 0.751 | 0.763 | 0.769 |
| 100 | 0.651 | 0.665 | 0.676 | 0.682 |
| 125 | 0.574 | 0.590 | 0.600 | 0.607 |
| 150 | 0.508 | 0.523 | 0.534 | 0.540 |
| 175 | 0.448 | 0.466 | 0.475 | 0.482 |
| 200 | 0.398 | 0.416 | 0.425 | 0.432 |
| 225 | 0.353 | 0.370 | 0.381 | 0.386 |
| 250 | 0.314 | 0.331 | 0.341 | 0.346 |

Table 3

Percentage differences between *TMR* measured with the stereotactic diode and with the PinPoint chamber.

| Depth (mm) | 5 mm | 10 mm | 12.5 mm | 15 mm |
|------------|------|-------|---------|-------|
| 5 | 7.0 | 1.8 | 3.1 | 0.7 |
| 8 | 2.1 | -0.2 | 0.5 | 5.6 |
| 12 | 1.0 | 0.1 | -0.1 | 0.7 |
| 14 | 0.3 | 0.1 | 0.0 | 0.3 |
| 15 | 0.0 | 0.0 | 0.0 | 0.0 |
| 16 | -0.1 | 0.1 | 0.1 | 0.1 |
| 18 | 0.2 | 0.2 | 0.0 | 0.2 |
| 20 | 0.2 | 0.3 | 0.0 | 0.0 |
| 25 | 0.4 | 0.5 | 0.2 | 0.3 |
| 30 | 0.4 | 0.0 | 0.2 | 0.2 |
| 40 | -0.1 | -0.4 | -0.6 | -0.3 |
| 50 | 0.4 | -0.7 | -0.5 | 0.0 |
| 75 | 0.6 | 0.1 | -0.1 | 0.3 |
| 100 | 1.6 | 0.5 | 0.3 | 0.0 |
| 125 | 1.4 | 0.5 | 0.3 | 0.8 |
| 150 | 1.7 | 0.8 | 0.7 | 0.8 |
| 175 | 1.4 | 0.9 | 0.8 | 0.9 |
| 200 | 1.6 | 1.1 | 1.2 | 0.8 |
| 225 | 1.5 | 0.1 | 1.2 | 0.7 |
| 250 | 1.3 | 0.4 | 1.1 | 0.7 |

In the *TMR* acquisition mode, the detector is located at a fixed position and always sees the same collimator opening, so there is no change of detector response with field size. This makes the use of the ionization chamber a good choice, in spite of its larger volume. Our *TMR* measurements with stereotactic diode and PinPoint 3D microionization chamber

Table 4

Percentage differences between calculated and measured *TMR* with stereotactic diode.

| Depth (mm) | 5 mm | 10 mm | 12.5 mm | 15 mm |
|------------|------|-------|---------|-------|
| 0 | -9.2 | 0.2 | 10.0 | 6.5 |
| 5 | -1.1 | -6.8 | -5.3 | -7.7 |
| 8 | -0.4 | -3.7 | -2.8 | 1.2 |
| 12 | -0.1 | -0.6 | -0.7 | -0.2 |
| 14 | 0.0 | -0.2 | -0.2 | -0.1 |
| 15 | 0.0 | 0.0 | 0.0 | 0.0 |
| 16 | 0.0 | 0.3 | 0.4 | 0.2 |
| 18 | 0.2 | 0.6 | 0.5 | 0.9 |
| 20 | 0.4 | 0.8 | 0.9 | 0.9 |
| 25 | 0.7 | 1.1 | 1.1 | 1.5 |
| 30 | 0.4 | 0.7 | 1.0 | 1.3 |
| 40 | 0.3 | 0.7 | 0.2 | 1.2 |
| 50 | 1.0 | 0.8 | 0.9 | 1.2 |
| 75 | 1.4 | 2.2 | 1.9 | 2.3 |
| 100 | 2.8 | 3.3 | 2.7 | 2.2 |
| 125 | 3.0 | 3.3 | 2.6 | 3.4 |
| 150 | 4.3 | 4.0 | 3.8 | 3.8 |
| 175 | 4.4 | 4.9 | 4.8 | 4.7 |
| 200 | 5.6 | 5.9 | 5.0 | 4.3 |
| 225 | 5.6 | 6.0 | 5.9 | 5.5 |
| 250 | 7.3 | 6.3 | 6.4 | 5.5 |

Table 5
Output factor curve.

| Diameter (mm) | Output factor |
|---------------|---------------|
| 5 | 0.712 |
| 10 | 0.834 |
| 12.5 | 0.873 |
| 15 | 0.891 |

agree very well. We used the chamber in combination with polystyrene and plate-mark positioning. On the other hand, *TMR* measured in water have a larger uncertainty in the depth of water added to the phantom. The diode was positioned with 2 orthogonal profiles acquired in scanning mode. Although this is a superior way of positioning, we reached good agreement between the 2 sets of measurements.

With respect to the *TMR* and *PDD* measurement in the buildup region, extrapolation chambers and well-guarded fixed separation plane parallel chambers are the recommended detectors in the International Atomic Energy Agency TRS-398¹² for measuring depth curves instead of cylindrical chambers. A note of caution is also given in this document with respect to the use of diodes. The context of this document is not small-field dosimetry. Specifically, in small fields, IPeM² recommends the use of plane parallel chambers for measuring depth curves. Unfortunately, the volume of most plane parallel chambers is too large to measure small fields, and this reason made our selection of the stereotactic detector and the microionization PinPoint chamber the best choice for this task, in spite of their limitations.

We used our stereotactic diode data as our gold standard and input data in the TPS for measured *TMR*, *OF*, and profiles, based on the recommendations of Refs. 2, 8 and the advice of Refs. 4, 6. They have a smaller volume effect, and the amount of perturbation is lower than with ionization chambers, as can be seen in Monte Carlo-calculated correction factors from Ref. 4 and Ref. 6. We also attributed the 3.5% difference between the stereotactic diode and the PinPoint microionization chamber in the measurement of the *OF* to the latter's higher volume effect that results in a change of response with the field size.

Conclusion

We have described our commissioning of a set of small field size radiosurgery cones in FFF beams. The procedures we followed are essentially the same as those used in the commissioning of small field size cones in flattened beams. The Stealth transmission chamber overcomes the problem of getting a strong reference signal when measuring very

small-size radiation fields. We have used it to measure *PDD* and profiles, and to get 2 orthogonal profiles to center a stereotactic diode to acquire *TMR*. Good agreement was found between measured *TMR* with PinPoint microionization chamber in polystyrene and stereotactic diode in water. Water measurements have a better centering, but the uncertainty in the depth of water is larger. Profiles and *OF* were measured with the stereotactic diode.

Acknowledgments

José Luis Roldán and Salih Arican, from IBA Dosimetry, are gratefully acknowledged for providing the Stealth Chamber and its technical data. The authors acknowledge the financial support from the Spanish “Ministerio de Economía y Competitividad (Instituto de Salud Carlos III)” (project PI16/00899) and the European Regional Development Fund (ERDF).

References

1. Das, I.J.; Ding, G.X.; Ahnesjö, A. Small fields: Non equilibrium radiation dosimetry. *Med. Phys.* **35**(1):206–15; 2008.
2. Institute of Physics and Engineering in Medicine. Small field MV photon dosimetry. IPeM Report Number 103; 2010.
3. Alfonso, R.; Andreo, P.; Capote, R.; et al. A new formalism for reference dosimetry of small and nonstandard fields. *Med. Phys.* **35**(11):5179–86; 2008.
4. Francescon, P.; Cora, S.; Satariano, N. Calculation of $k_{Q_{clin}, Q_{msr}}^{f_{clin}, f_{msr}}$ for several small detectors and for two linear accelerators using Monte Carlo simulations. *Med. Phys.* **38**(12):6513–27; 2011.
5. Bouchard, H.; Seuntjens, J.; Duane, S.; et al. Detector dose response in megavoltage small photon beams. I. Theoretical concepts. *Med. Phys.* **42**(10):6033–61; 2015.
6. Lechner, W.; Palmans, H.; Sölkner, L.; et al. Detector comparison for small field output factor measurements in flattening filter free photon beams. *Radiother. Oncol.* **109**:356–60; 2013.
7. Das, I.J.; Cheng, C.W.; Watts, R.J.; et al. Accelerator beam data commissioning equipment and procedures: Report of the TG-106 of the Therapy Physics Committee of the AAPM. *Med. Phys.* **35**(9):4186–215; 2008.
8. European Society for Radiotherapy and Oncology. Guidelines for the Verification of IMRT. 2008. ESTRO Booklet no. 9.
9. Gersh, J.A. Stereotactic beam characterization using the IBA Stealth reference detector. IBA Dosimetry White paper 2014.
10. Khan, F.M. The Physics of Radiation Therapy. 5th ed. Philadelphia, PA: Wolters Kluwer–Lippincott Williams and Wilkins; 2014.
11. Khan, F.M.; Sewchand, W.; Lee, J.; et al. Revision of tissue-maximum ratio and scatter maximum ratio concepts for cobalt 60 and higher energy x-ray beams. *Med. Phys.* **7**:230–7; 1980.
12. Andreo, P.; Burns, D.T.; Hohlfield, K.; et al. Absorbed dose determination in external beam radiotherapy: An international code of practice for dosimetry based on standards of absorbed dose to water. International Atomic Energy Agency (IAEA) Technical Report Series 398, 2000.